

## RESEARCH ARTICLE

Editorial Process: Submission:04/30/2024 Acceptance:08/11/2024

# LncRNA TMPO-AS1 Promotes Triple-Negative Breast Cancer by Sponging miR-383-5p to Trigger the LDHA Axis

Prerna Vats<sup>1</sup>, Jai Singh<sup>1</sup>, Sandeep K. Srivastava<sup>1</sup>, Ashok Kumar<sup>2</sup>, Rajeev Nema<sup>1\*</sup>

## Abstract

**Background:** Understanding the heterogeneous nature of breast cancer, including the role of *LDHA* expression regulation via non-coding RNAs in prognosis, is still unknown, highlighting the need for more research into its molecular roles and diagnostic approaches. **Methods:** The study utilized various computer tools to analyze the differences between *LDHA* in tissues and cancer cells. It used data from TIMER 2.0, UALCAN, and TISIDB to study gene expression and survival outcomes in breast cancer patients. The study also used the Breast Cancer Gene Expression Miner to examine the relationship between *LDHA* gene expression and breast cancer type. Other tools included TCGAPortal, TNMplot, ctcRbase, GSCA, Enrichr, TISIDB, Oncomx, and TANRIC. The study then explored the relationship between tumor-infiltrating immune cells and *LDHA* formation using the GSCA and TISIDB repositories. We used Auto Dock Tools 1.5.6 to perform ligand binding analysis for *LDHA*, withanolides, and the known inhibitor LDH-IN-1. LigPlot+ and Pymol were used for visualization of protein-ligand complexes. **Results:** *LDHA* overexpression in breast cancer cells, metastatic tissue, and circulating tumor cells leads to shortened recurrence-free survival, overall survival, and distant metastasis-free survival. In invasive breast cell carcinoma, we observed that *LDHA/HIF-1 $\alpha$ /TMPO-AS1* are overexpressed while miR-383-5p is downregulated. This overexpression is associated with poor prognosis and may lead to Act<sub>DC</sub> infiltration into the tumor microenvironment. Withanolides, viz., Withaferine A and Withanolide D, have shown high binding affinity with *LDHA*, with binding energies of -9.3kcal/mol and -10kcal/mol respectively. These could be attractive choices for small-molecule inhibitor design against *LDHA*.

**Keywords:** *LDHA*- lncRNA- miRNA- UALCAN- Kaplan-Meier Plot- Prognosis for Breast Cancer- Auto Dock

*Asian Pac J Cancer Prev*, 25 (8), 2929-2944

## Introduction

Breast cancer is a global disease with 1.7 million new cases and 500,000 deaths, mostly resulting from metastasis that hinders further treatment [1]. Triple-negative breast cancer (TNBC) patients have worse outcomes due to a higher rate of metastasis compared to non-TNBC patients [2]. Standard cytotoxic chemotherapy and radiotherapy are the only treatments for TNBC patients, but these treatments are ineffective, and a significant (35%–40%) relapse occurs within 5 years after diagnosis [3]. Many drugs targeting angiogenesis, DNA repair, growth, and epigenetic modification have been evaluated, but clinical results are promising. Breast cancer is a complex disease with diverse histological and molecular expression profiles, risk factors, and clinical courses. Advances in molecular gene expression profiling have led to the emergence of different molecular subclassification systems with different clinical outcomes [4]. DNA microarray analysis classified breast cancer into Luminal A, Luminal B, *HER2*-positive, basal-like, and normal-like subtypes

[3]. A new molecular hunter is needed for treatment decisions, especially in advanced patients where treatment is limited and palliative. [5]. Lactate dehydrogenase (LDH) is an enzyme that plays an important role in anaerobic glycolysis and glycolysis. It influences cancer patients [6]. The human genome contains four LDH genes: *LDHA*, *LDHB*, *LDHC*, and *LDHD* [7]. Metabolic changes are important features of many cancers and can predict their onset and progression. Cancer cells prefer anaerobic glycolysis over mitochondrial oxidative phosphorylation and produce glycolytic intermediates and lactate as another fuel [7]. High levels of LDH in cancer cells indicate that cells are more resistant to chemotherapy and radiation, leading to poor outcomes [8]. *LDHA* is associated with various types of cancer in humans, including pancreatic cancer [9], laryngeal squamous cell carcinoma [10], cancer of the head and neck [11], kidney cancer [12], stomach cancer, prostate cancer [13], breast cancer [14], hepatocellular carcinoma [15], oral squamous cell carcinoma (OSCC) [16], and hematopoietic cancer [17]. Inhibiting *LDHA* can reduce

<sup>1</sup>Department of Bioscience, Manipal University Jaipur, University Jaipur, Dehmi Kalan, Jaipur-Ajmer Expressway, Jaipur, Rajasthan, 303007, India. <sup>2</sup>Department of Biochemistry, All India Institute of Medical Sciences (AIIMS), Bhopal, Saket Nagar, Bhopal 462 020, Madhya Pradesh, India. \*For Correspondence: rajeev.nema@jaipur.manipal.edu

tumor proliferation, migration, invasion, angiogenesis, and cancer metastasis and increase the sensitivity of cancer cells to chemotherapy and radiotherapy [8]. Tamoxifen resistance is associated with decreased ATP production and increased tumor glycolysis, resulting in the induction of autophagy [18]. Epithelial mesenchymal transition (EMT) development and metastasis in prostate cancer are associated with overexpression of *LDHA* and immunosuppression of CPTII, highlighting the importance of pharmacological inhibition in reducing EMT development [19]. *LDHA* expression is important in hypoxic states and pancreatic ductal adenocarcinoma [20]. Despite the recognition of *LDHA*'s significance, current inhibitors available, such as FX-11, Gossypol, Oxamata, and Galloflavin, are mostly chemical or synthetic-based [21]. Researchers are exploring natural product-based compounds like withanolides, derived from *Withania somnifera*, as a substitute for chemical-based inhibitors due to their potential to have fewer side effects and greater bioavailability as they address limitations such as toxicity and drug resistance [22]. Withanolides have various pharmacologic properties, including adaptogenic, diuretic, anti-inflammatory, sedative/anxiolytic, cytotoxic, antitussive, and immunomodulatory effects [23]. Understanding the relationship between *LDHA* reporting status and prognosis is crucial for cancer patient survival and recurrence. Long-non-coding RNAs (lncRNAs) play a significant role in cancer metastasis, regulating processes like the epithelial-mesenchymal transition. Thousands of lncRNAs have abnormal expression or mutations in various cancer types, acting as competitive-endogenous RNAs (ceRNAs) by engaging with microRNAs. Keeping all these problems in mind, the study aims to investigate the expression levels of TMPO-AS1, miR-383-5p, and the *LDHA*-mediated hypoxia signaling pathway in *BRCA* samples in order to create non-invasive molecular markers for improved breast cancer surveillance using publicly available datasets. This work also aims to find a selective molecule, such as withanolide (withanolide D + NADH, withaferin A + NADH, withanolide O + NADH, withanolide E + NADH, withanolide G + NADH, and withasomnine +NADH), that targets breast cancer via nanoliposome encapsulation and *LDHA* overexpression. The efficacy of these withanolide compounds was compared with a well-known inhibitor of *LDHA*, i.e., LDH-IN-1, which was employed in a study done by Liu et al., in which they suppressed the expression of *LDHA* using LDH-IN-1 in colorectal cancer [24].

## Materials and Methods

### Expression Analysis of *LDHA*

Initially, the expression of *LDHA* was assessed in pan-cancer by using the UALCAN database (<http://ualcan.path.uab.edu/>), which is a publicly available cancer database [25], TIMER 2.0 [26] (<http://timer.cistrome.org/>), and the TISIDB database (<http://cis.hku.hk/TISIDB/index.php>) [27]. Additionally, we analyzed differences in *LDHA* mRNA expression patterns in cancer patients using OncoDB (<https://oncodb.org/>) [28], GEPIA2 (<http://gepia.cancer-pku.cn/>) [29], and ENCORI (<https://rnasysu.com/encori/index.php>) [30] databases.

We used Breast Cancer Gene Expression Miner v5.0 (<http://bcgenex.unicancer.fr/>) [31] to examine the relationship between *LDHA* expression value and patient clinicopathological characteristics such as hormone receptor status (ER and PR), *HER2*, Basal-like and TNBC pathological subtypes, further validation of the *BRCA* subtype was done by using TISIDB, TCGA Portal (<http://tumorsurvival.org/index.html>) [32], bc-GenExMinerv5.0, and UALCAN databases. TNMplot (<http://www.tnmplot.txt>) [33] was used to analyze the relationship of *LDHA* expression with metastasis and the ctcRbase database (<http://www.origin-gene.cn/database/ctcRbase/>) [34] was used to validate the result. Protein Analysis was done using Protein Atlas (<https://www.proteinatlas.org/>) [25].

### Survival Analysis

Survival analysis was performed on breast cancer data using Kaplan-Meier Plotter (<https://kmlot.com/analiz/>) [35]. The filters are: "Cancer: Breast Cancer"; "Gene Symbol: *LDHA*"; Affy ID: 200650\_s\_at, *HIF1A*; In 200989\_PGK1; 227068\_at, PPIA; 226336\_at, T, Gsp10PI410\_20; 209251\_x\_at, VDAC1: 212038\_s\_at and PSMD14; 212296\_at, survival: recurrence-free survival (RFS), overall survival (OS) and distant metastasis-free survival (DMFS) and distribution of patients by median and JetSet evaluation at most.

### Functional Heterogeneity and Transcriptional Factor Analysis

CancerSEA is a unique database that examines different functions of cancer cells at the cellular level (<http://biocc.hrbmu.edu.cn/CancerSEA/home>) [36]. It describes the functional state map of an individual cancer, which includes 14 functional states (such as stem cells, invasion, metastasis, proliferation, EMT, angiogenesis, apoptosis, cell cycle, differentiation, DNA damage, DNA repair, hypoxia, inflammation, and more). CancerSEA was used to determine the relationship of *LDHA* gene expression to different biological processes. Further, GEPIA2, TIMER, and OncoDB databases were used to find the correlation between *LDHA* and the transcriptional factor.

### Co-expressed Functional Enrichment Analysis

The Enrichr database (<https://maayanlab.cloud/Enrichr/>) [37] was used to identify *LDHA* co-expressed genes, and the GSCALite database (<http://bioinfo.life.hust.edu.cn/web/GSCALite/>) was further utilized to validate the co-expressed genes in breast cancer [38]. Finally, the *LDHA* gene ontology was analyzed using the TISIDB database. Furthermore, we used TNMplot to assess the co-expressed genes for metastatic function, and then we used TIMER 2.0 to investigate the relationship of the *LDHA* gene with the co-expressed genes.

### Non-coding-Regulatory Network Analysis

We used the GSE55807, GSE41245, and GSE75367 ctcRbase datasets to identify miRNAs targeting the *LDHA* gene. UALCAN and GSCA were used for validation. Additionally, UALCAN and KM plotter were used to

evaluate the significance of *LDHA*-related miRNAs with pathological conditions. Non-Coding RNA Cancer Atlas (TANRIC, <http://bioinformatics.mdanderson.org/main/TANRIC:Overview>) [39], UALCAN and ENCORI libraries were used to control lncRNA analysis.

#### Tumor-Infiltrating Immune Cells (TIICs) Analysis

TISIDB (<http://cis.hku.hk/TISIDB/index.php>) [40] and GSCA (<http://bioinfo.life.hust.edu.cn/GSCA/#/>) [41] are interactive web applications that analyze TCGA data to correlate *LDHA* expression with tumor-immune cells, providing valuable insights into TIICs (M1 macrophages, M2 macrophages, M0 macrophages, T follicular helper cells, resting memory CD4 T cells, activated memory CD4 T cells,  $\gamma\delta$  T cells, CD8 T cells, regulatory T cells, naive CD4 T cells, resting NK cells, activated NK cells, resting mast cells, activated mast cells, memory B cells, resting dendritic cells, activated dendritic cells, naive B cells, monocytes, neutrophils, eosinophils, and plasma cells) in breast cancer subtypes. The Spearman correlation was adjusted using tumor purity. P-values of <0.05 or less are considered statistically significant.

#### Protein and ligand data acquisition

The three-dimensional crystal structures of Lactate Dehydrogenase A (*LDHA*) from *Homo sapiens* (PDB ID: 5W8L) was retrieved from the Protein Data Bank (<https://www.rcsb.org>) [42]. The structure was prepared for molecular docking by removing water molecules and three chains by using pymol software [43] that results into only chain A was left for molecular docking studies. Ligand binding site was retrieved by analysing the various Lactate Dehydrogenase A (*LDHA*) and inhibitor complexes available in PDB. The chemical structures of ligand were retrieved from PubChem database (<http://PubChem.ncbi.nlm.nih.gov>) [44] and all six ligands were: Withanolide D, Withaferine A, Withanolide O, Withanolide E, Withanolide G, Withasomnine. The structure minimization was carried out by UCSF Chimera [45] with the 1000 steepest descent steps, followed by addition of Gasteiger charges and polar hydrogen atoms.

#### Protein-ligand Molecular Docking

To comprehend the binding interactions of ligands with *LDHA* protein, a molecular docking analysis was conducted using the Auto Dock Tools 1.5.6 (ADT) [46]. Gasteiger partial charges were assigned to the ligand atoms after including the electron density contributed by non-polar hydrogen bonds and ligand torsions. Other than that, the Kollman charges were used for the protein incorporating the influence of polar hydrogen atoms. The calculation of both charges and solvation parameters was performed using AutoDock Tools module. The protein binding sites were explored by Auto Dock 4.2 [47], Lamarckian Genetic Algorithm (LGA). A grid of 70×70×70 points along x, y, z direction with a 0.375 Å grid spacing centred with the dimensions along x, y, and z as -17.9, 39.24, and -40 Å. Ten docked conformations were generated for each ligand as the number of genetic algorithm runs was 10 and ligands were ranked according to their docking scores. The top two hits whose docking

score is greater than the known inhibitor was selected for further validation. The protein-ligand complex was visualized using UCSF Chimera and LigPlot+ [48].

#### Statistical Analysis

Differences in *LDHA* gene expression between tumor and normal tissues were analyzed by t test. The relationship between *LDHA* gene expression and prognosis was analyzed with an online model. Survival, *LDHA* performance heterogeneity and gene enrichment between the two groups were compared using Log-Rank tests. Statistical significance is  $P < 0.05$ . Validity data were analyzed through statistical analysis based on online databases.

## Results

### *LDHA* Expression in Human Breast Cancer: A Pan-Cancer Approach

First, we analyzed *LDHA* expression in all TCGA cancers, including breast cancer, using UALCAN, TIMER, TCGA-Portal and ONCOMX databases to assess cancer differentiation. The results showed that the amount of *LDHA* expressed in tissues of malignant tumors was generally higher than in normal tissues (Figure 1A-C and Supplementary Table 1). Importantly, as shown in Figure 2A, TCGA analysis of UALCAN expression data showed that *LDHA* gene expression was increased in tumors from cancer patients, with an average ninefold upregulation compared to normal tissues ( $p < 1e-12$ ). Using TCGAportal ( $P < 0.05$ ), ENCORI ( $P = 2.9e-12$ ), GEPIA2 ( $P < 0.05$ ), and OncoDB databases ( $P = 2.8e-19$ ), similar patterns of overexpression were revealed in tumor patients, as shown in Figure 2B-E. Additionally, the prognostic role of the *LDHA* gene in cancer was examined using the KM Plotter database, comparing the survival outcomes of patients with high and low *LDHA* expression levels, and reviewing its relationship with survival rates, and we found that the *LDHA* expression level was high. *LDHA* expression levels are associated with poor prognosis in breast cancer patients. Side effects for cancer patients were Relapse-free survival (RFS) (HR = 1.48, 95% CI: 1.34-1.65,  $P = 5.3e-14$ ) and overall survival

Table 1. *LDHA* and its Co-Expressed Genes

Cancer Type	Gene Symbol	FC
BRCA	<i>EIF2S1</i>	1.11861
	<i>ENO1</i>	1.217615
	<i>HIF1A</i>	1.291856
	<i>LDHA</i>	1.508099
	<i>PGK1</i>	1.926633
	<i>PPIA</i>	1.52508
	<i>PSMD14</i>	1.810576
	<i>RAN</i>	1.677762
	<i>TPI1</i>	1.707963
	<i>TUBA1C</i>	2.863197
	<i>VDAC1</i>	1.524079
	<i>VDAC2</i>	1.081065



Table 2. *LDHA* associated miRNAs

miRNA Name	PITA	miRanda	RNAhybrid
hsa-miR-149-5p	Yes	Yes	No
hsa-miR-30a-5p	Yes	Yes	No
hsa-miR-30b-5p	Yes	Yes	No
hsa-miR-30c-5p	Yes	Yes	No
hsa-miR-30d-5p	Yes	Yes	No
hsa-miR-30e-5p	Yes	Yes	No
hsa-miR-323a-3p	Yes	No	Yes
hsa-miR-338-3p	Yes	Yes	No
hsa-miR-33a-5p	Yes	Yes	Yes
hsa-miR-33b-5p	Yes	Yes	Yes
hsa-miR-34a-5p	Yes	Yes	Yes
hsa-miR-34c-5p	Yes	Yes	Yes
hsa-miR-383-5p	Yes	Yes	Yes
hsa-miR-410-3p	Yes	Yes	No
hsa-miR-449a	Yes	Yes	Yes
hsa-miR-449b-5p	Yes	Yes	Yes
hsa-miR-501-3p	Yes	No	Yes
hsa-miR-502-3p	Yes	No	Yes
hsa-miR-7-5p	Yes	Yes	No
hsa-miR-876-5p	Yes	No	Yes

(OS) (HR = 1.35 , 95%) was significantly related to CI: 1.11-1.64,  $P = 0.0023$ ) and distant metastasis-free survival (DMFS) (HR = 1.23, 95% CI: 1.05-1.44,  $P = 0.01$ ), as shown in Figure 2F-H. These data suggest that *LDHA* is a poor indicator of breast cancer.

#### Correlation of *LDHA* expression with ER, PR, and HER2

The study then evaluated breast cancer cells, including ER+/ER-, PR+/PR-, and HER2+/HER2, to determine the effect of *LDHA* in relation to specific subtypes. The expression of *LDHA* in metastases was compared with the bc-GenExMiner 5.0 database. Subsequently, hormone receptor-negative tumor subtypes expressed more *LDHA* than hormone receptor-positive subtypes, as shown in Figure 3A-D. *LDHA*, was found to be associated with ER- ( $p = 0.0001$ ), PR- ( $p = 0.0001$ ), ER-/PR- ( $p = 0.0001$ ), and HER2+ ( $p = 0.0001$ ). In addition, we also compared the effectiveness of *LDHA* between non-basal-like and basal-like and non-TNBC and TNBC. As shown in Figure 3E-F, significantly greater ( $p = 0.0001$ ) *LDHA* expression was found in basal-like and TNBC subtypes compared to non-basal-like and non-TNBC subtypes. We also investigated the expression of the *LDHA* gene in breast cancer cells (Luminal A, Luminal B, Basal, and Her2) using TISIDB, TCGAportal, and bc-GenExMiner databases, as shown in the Figure 3G-I, and found that it is highly expressed in breast cancer subtypes. Additionally, we analyzed the above data using UALCAN and found that *LDHA* activity was more closely related to the aggressiveness of breast cancer: Normal vs. luminal ( $P = <1e-12$ ), normal vs. HER2+ ( $P = 5.3e-04$ ), and  $P = 9.1e-12$  for normal versus TNBC, as shown in Figure 3J.

Table 3. *LDHA*'s Binding Affinity with Ligands

Ligands	Binding energy (Kcal/mol)
Withanolide D +NADH	-10
Withaferine A + NADH	-9.3
Withanolide O + NADH	-9.1
Withanolide E + NADH	-8.9
Withanolide G +NADH	-8.9
Withasomnine +NADH	-6.3

#### Metastasis and circulating tumor cells are associated with *LDHA* Expression

To determine *LDHA*'s role in metastasis, we analyzed gene expression in tumors from breast cancer patients by using TNMplot database (Gene Chip), which showed significantly higher *LDHA* expression than normal-metastatic tissue ( $P = 1.38e-12$ ) as shown in Figure 4A, Further the ctcRbase database confirmed the *LDHA* gene's involvement in metastasis as shown Figure 4B, also, Figure 4C illustrates that *LDHA* expression is highly associated with circulating tumor cells (CTCs).

#### An analysis of the heterogeneity and gene enrichment of *LDHA* expression and transcription factors

According to CancerSEA data, there is a strong association between *LDHA* gene expression and hypoxia ( $r=0.60$ ), as shown in Figure 5A, illustrating hypoxia-related mechanisms. It is well known that hypoxia-induced transcription factors can affect tumor growth. The GEPIA2 database was used to explore if the *LDHA* gene is connected with genes that govern hypoxia. A substantial correlation was observed between the two genes hypoxia inducing factor 1- $\alpha$  (*HIF1A*) and *LDHA*, with a correlation value of 0.41 and a p value of  $<0$ , as shown in Figure 5B. Interestingly, the study used TIMER to identify the relationship between the *HIF1A* and *LDHA* genes, which showed a significant correlation of 0.36 and a p value of  $2.5e-36$  in Figure 5C, and a similar data was found out using OncoDB which showed the correlation value to be 0.34 and  $P$  value =  $2.01e-33$  as shown in Figure 5D. This study also examined the *HIF1A* gene's prognostic significance in breast cancer using the KM Plotter database. Results showed that breast cancer patients with high *HIF1A* expression improved significantly, including relapse-free survival (RFS) (HR = 1.39, 95% CI: 1.26-1.54,  $P = 1.6e-10$ ) and overall survival (OS) showed that it had a poor prognosis (HR = 1.58, 95% CI: 1.31-1.92,  $P = 1.9e-06$ ), distant metastasis-free survival (DMFS) (HR = 1.21, 95% CI: 1.04-1.41,  $P = 0.016$ ), and post-progression survival (PPS) (HR = 1.84, 95% CI: 1.45-2.33,  $P = 2.8e-07$ ), as shown in Figure 5E-H. These data suggest that *HIF1A* is a negative marker of cancer. The Enrichr database was used to identify associated genes to understand the molecular mechanisms underlying the association between the *LDHA* gene and cancer. Ten genes were found to be associated with *LDHA*, specifically *EIF2S1*, *ENO1*, *VDAC1*, *VDAC2*, *PGK1*, *PPIA*, *PSMD14*, *RAN*, *TPII*, and *TUBA1C*. These gene were further validated using the TIMER 2.0 database, and the data showed a strong association between *LDHA* and the genes, indicating a specific association in cancer,

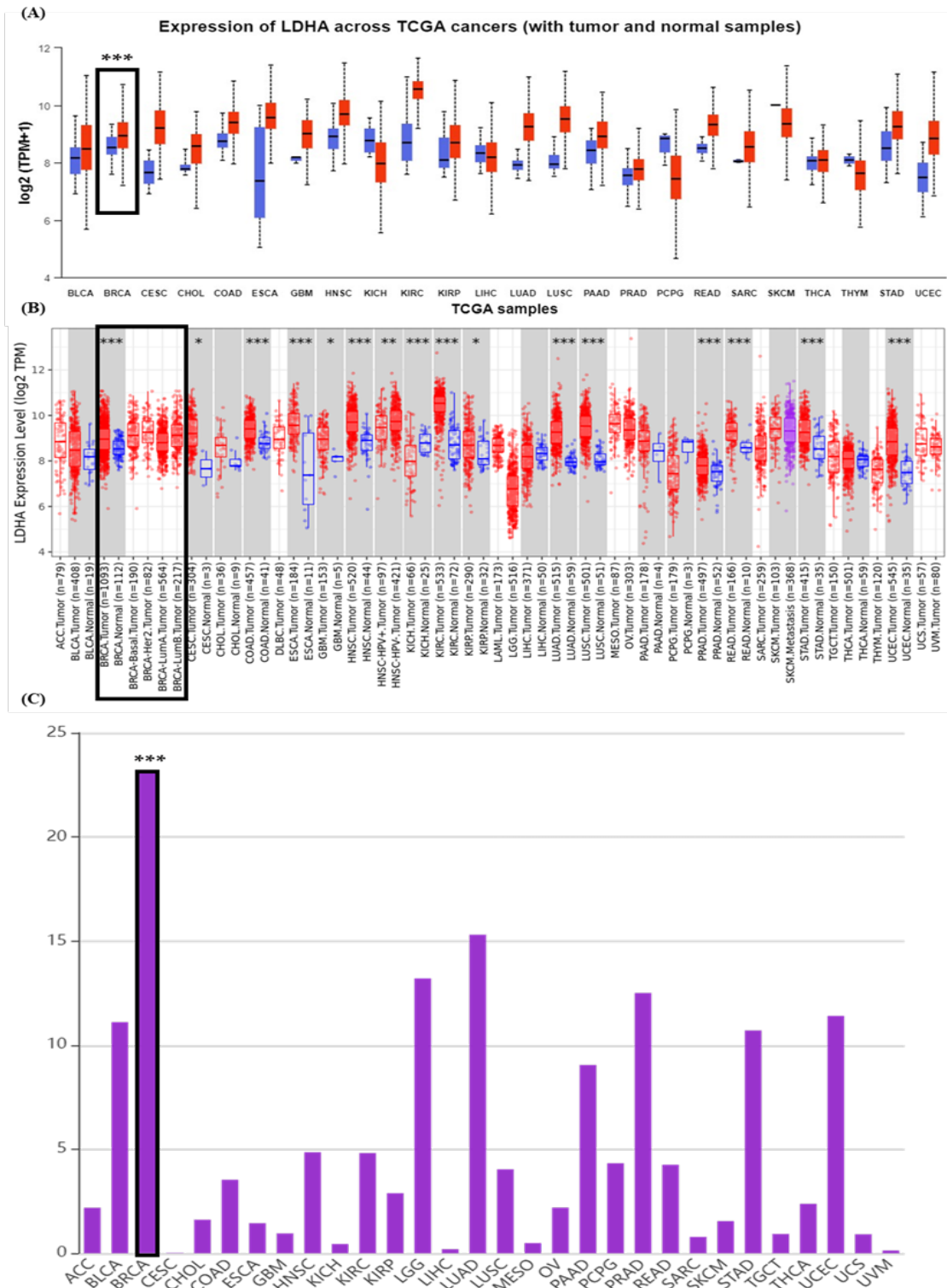


Figure 1. Expression Pattern of *LDHA* in Pan-Cancer (A) Expression profile of *LDHA* was determined by the UALCAN database for tumor versus normal samples; Red bars = Tumors, blue bars corresponding normal tissue. (B) expression of *LDHA* in pan-cancer by TIMER 2.0 meta-analysis; tumors compared with matched normal samples, Red bar-dot plot = Tumors, blue bar-dot plot corresponding normal tissue. Error bars represent SD. \*\*\* $p < 0.001$ . (C) expression of *LDHA* in different types of cancers by TISIDB database.

as shown in Figure 6A.

The study used the GSCA database to determine gene expression patterns in cancer patients and showed major log fold changes for each gene participant in case of *BRCA* as mentioned in Table 1. This study also examined the combined gene expression i.e. gene variant analysis

(GSVA) score of the co-expressed genes in tumor vs normal types and found a comparatively high expression in *BRCA* with a P value of  $5.09 \times 10^{-46}$ , further, expression level in patterns of breast cancer pathological subtypes Basal, Her2, LumA, LumB, and Normal, showed their association with aggressiveness with a p value of  $3.12 \times 10^{-42}$

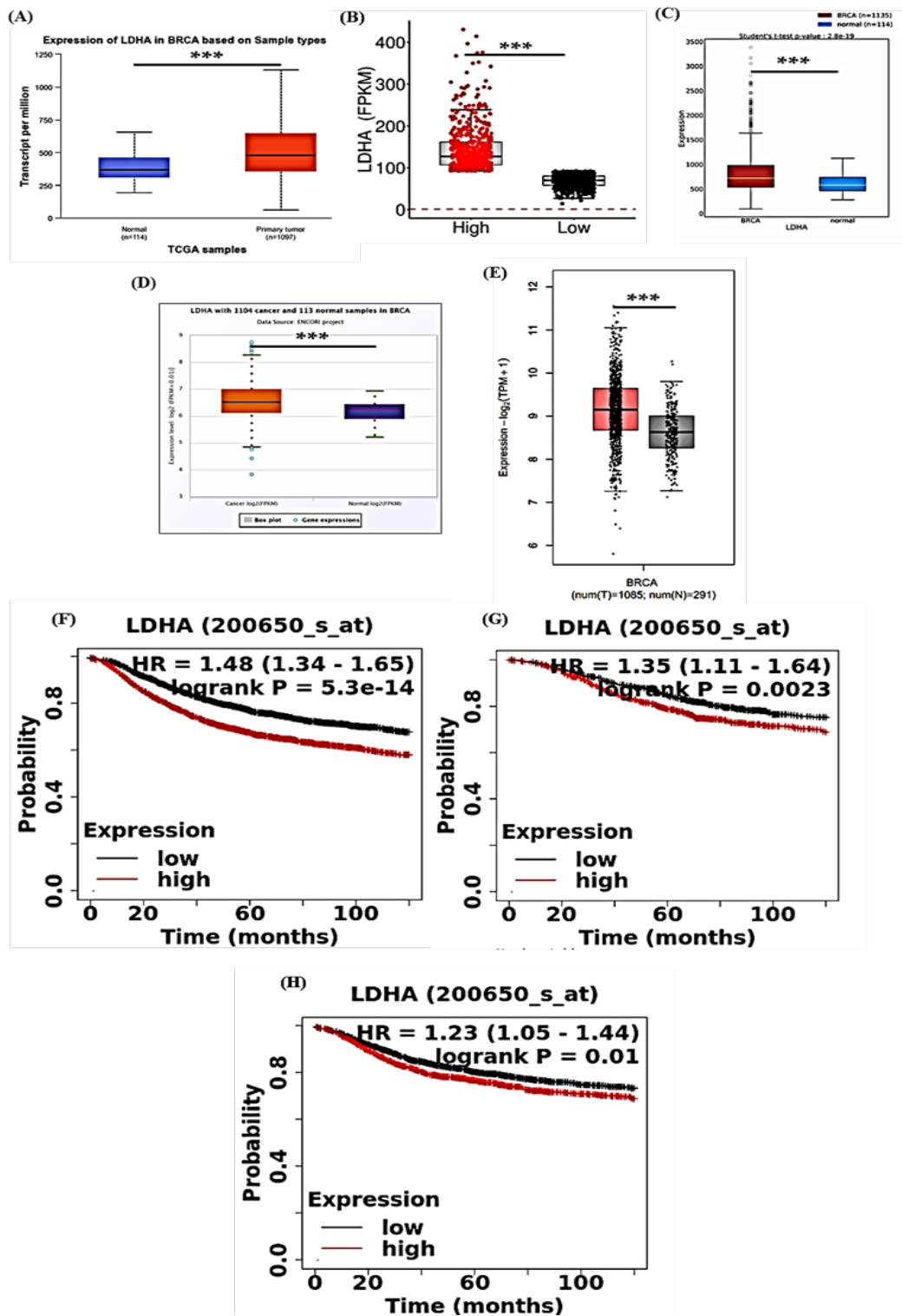


Figure 2. Expression of *LDHA* in Breast Cancer (A-E) mRNA expression was analyzed in normal breast tissue and primary tumors from the publicly available (A) UALCAN (Normal n= 114, Tumor n= 1097); (B) TCGA portal; (C) OncoDB (Normal n= 114, Tumor n= 1135); (D) ENCORI (Normal n= 113, Tumor n= 1104); and (E) GEPIA 2 (Normal n= 291, Tumor n= 1085) databases. (F-H) Prognostic role of mRNA expression of *LDHA* in breast cancer patients. Kaplan-Meier survival curves were plotted for (F) RFS (n=4929), (G) OS (n=1879), and (H) DMFS (n=2765).

as shown in Figure 6B-C. Additionally, UALCAN data showed that only *PGK1*, *PPIA*, *PSMD14*, *RAN TPII*, *TUBA1C*, and *VDAC1* were overexpressed in breast cancer patients compared with normal individuals, as shown in Supplementary Figure 1A–G. Additionally, the KM plotter database revealed that all seven genes, including *LDHA*

and *HIF1A* transcripts, were associated with poor survival in cancer patients. Data showed a significant association between these genes and breast cancer in RFS (HR = 1.87, 95% CI: 1.6-2.18, P = 7e-16) and OS (HR = 1.76, 95% CI: 1.34- 2.31), P = 4.1e-5) and DMFS (HR = 1.68, 95% CI: 1.29-2.2, P = 0.00012), respectively, as shown

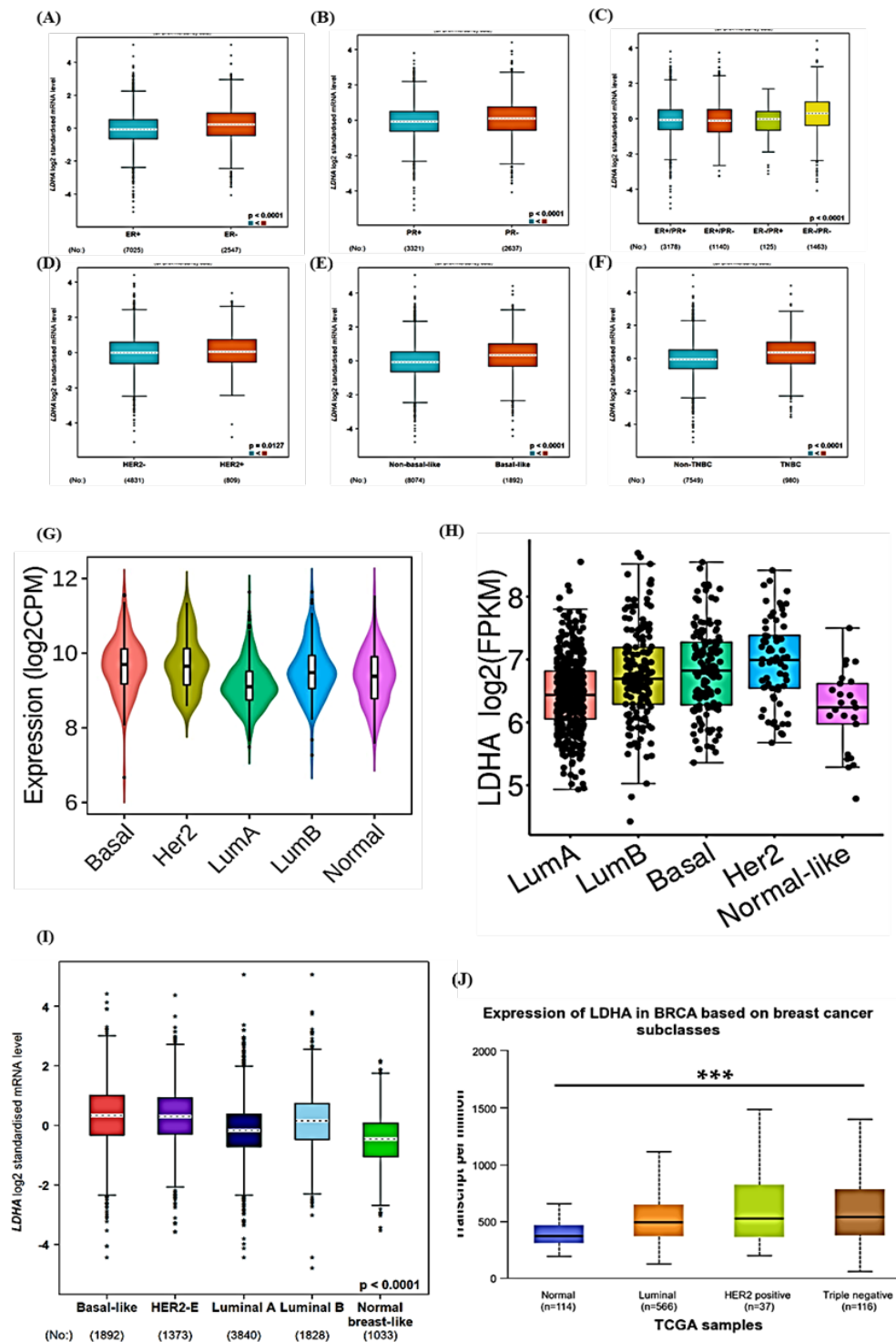


Figure 3. *LDHA* Expression in Tumor Tissues from Breast Cancer Patients with Various Clinicopathological Features Determined by the bc- GenExMiner Database. Boxplot of *LDHA* expression in tumor tissues from breast cancer patient's ER positivity status (A); with different PR positivity status (B); ER/PR status (C); *HER2* status (D); basal-like (E); and TNBC (F). Violinplot of *LDHA* expression in tumors from breast cancer patients with different histological subtypes analyzed by TISIDB (G); TCGA Portal (H); bc-GenExMiner (I); and UALCAN (Normal n=114, Luminal n=566, *HER2*+ n=37 and TNBC n=116) (J).

in Supplementary Figure 1H-J.

#### *LDHA* Expression Regulation by miRNAs

The overexpression of *LDHA* in breast cancer has been demonstrated in previous studies. However, the mechanisms underlying *LDHA* dysregulation in breast

cancer remain unclear. To search for *LDHA*-regulated microRNAs in breast cancer, we identified the top 20 *LDHA*-associated miRNAs using the ctcRbase library (Table 2 and Supplementary Figure 2). These miRNAs were validated using PITA, miRanda, and RNA hybrid libraries. Seven significant miRNAs were identified, including

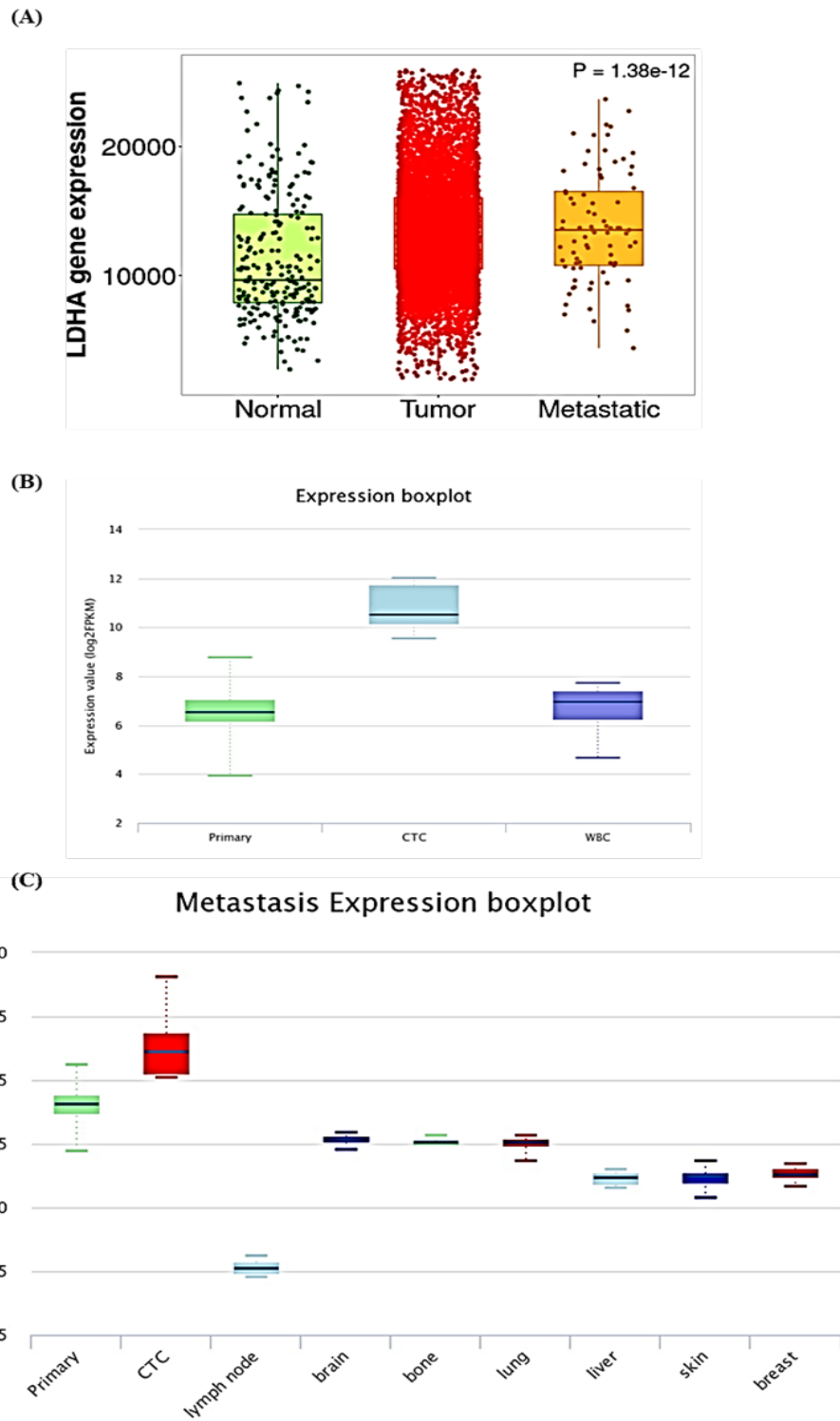


Figure 4. *LDHA* Expression in Tumors from Breast Cancer Patients with Metastasis. (A) Boxplot of *LDHA* expression between normal, tumor, and metastasis in breast cancer patients using the Gene Chip- TNMplot database; (B) Boxplot of *LDHA* expression in normal tissue, circulatory tumor cells (CTC); and secondary metastasis sites from breast cancer patients using ctcRbase database (C).

hsa-miR-33a-5p, hsa-miR-33b-5p, hsa-miR-34a-5p, hsa-miR-34c-5p, hsa-miR-383-5p, hsa-miR-449a, and hsa-miR-449b-5p. Using CancerMIRNome, the study found that miRNA miR-383-5p was negatively associated with cancer patients (coefficient  $R = -0.355$ ,  $P = 4.59e-14$ ), as shown in Figure 7A. Further, differential expression of miR-383-5p in tumor vs. normal using UALCAN,

CancerMIRNome, and ENCORI databases showed its downregulation in *BRCA* sample type as shown in Figure 7B-D. Additionally, UALCAN data was also used to analyze miR-383-5p expression in patients with different tumors, lymph nodes, and histological types. As shown in the Figure 7E-G, it presents a lower expression in the final stage of each pathological stage.



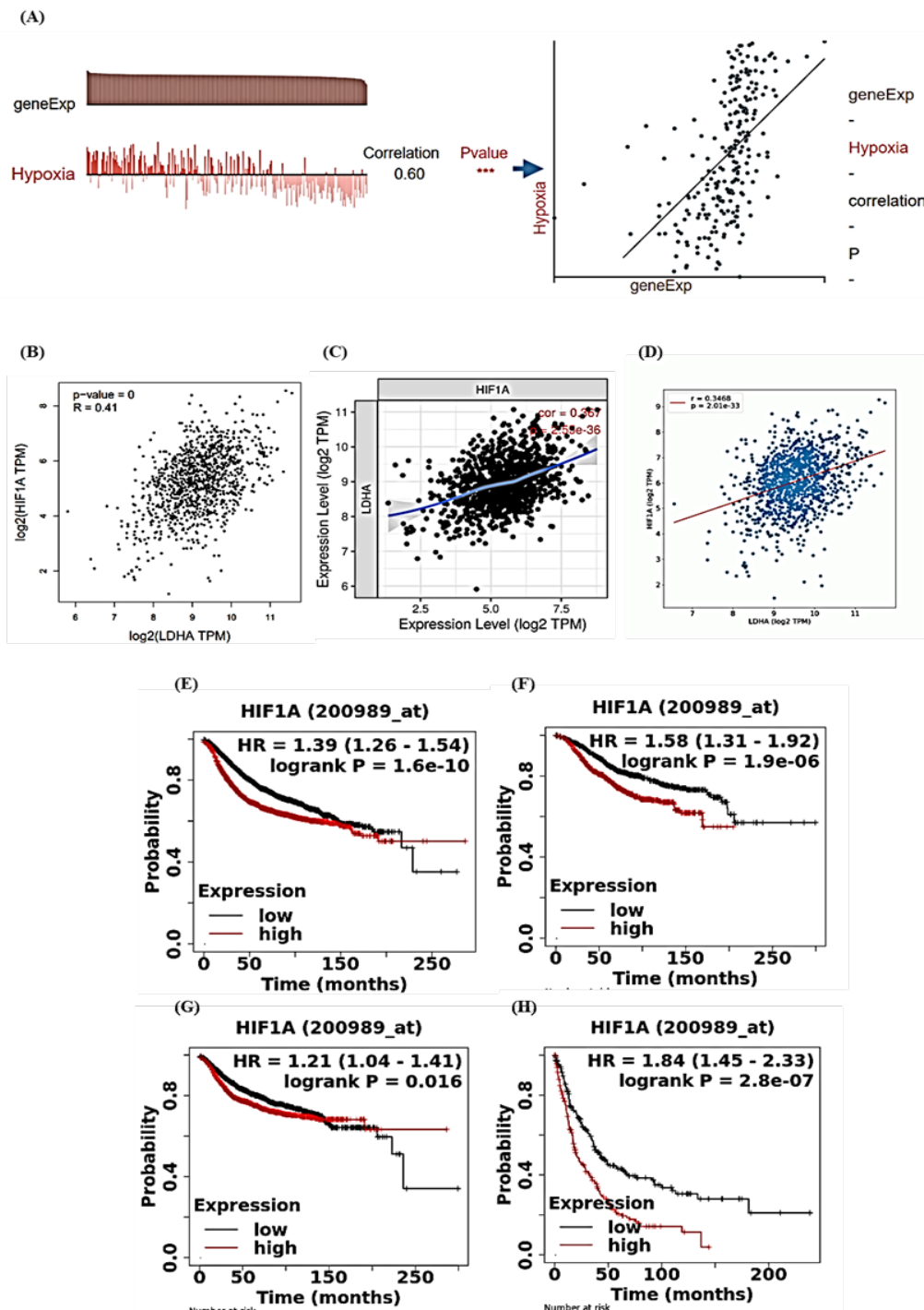


Figure 5. *LDHA* Expression and Molecular Functional States and Correlation (A) expression and its involvements in Hypoxia in breast cancer patients using the CancerSEA database. Expression correlation between *LDHA* Vs. *HIF1A* by using (B) GEPIA; (C) TIMER 2.0; and (D) ENCORI. (E-H) Prognostic role of mRNA expression of *HIF1A* in breast cancer patients. Kaplan-Meier survival curves were plotted for (E) RFS (n=4929), (F) OS (n=1879), (G) DMFS (n=2765), and (H) PPS (n=458).

#### Regulation of TNBC by the LncRNA *TMPO-AS1* and the miR-383-5p feedback loop

Epigenetic modification is crucial for gene regulation, transcription, and translation, and certain lncRNAs, such as *SPRY4-IT1*, *HOTAIR*, *TMPO-AS1*, *MALAT*, *DSCAM-AS1*, *BCAR4*, *BORG*, *HCP5*, *CASCAL 2*, *DANCR*, *LINC00922*, *ST8SIA6-AS1*, *ROR*, *LINC00461*, *LC-1S*, *NEAT*, *RP1*, *TINCR*, *LINP1*, *CRALA*, *TMPO-AS1*, *CYTOR*, *MIR2052HG*, *CCAT1*, *TROJAN*, *NRAD1*,

*DANCR*, *NAMPT-AS*, *linc-ZNF469-3*, *HULC*, *SONE*, *ARNILA*, *EPIC1*, *GACNT-1*, *ACID*, *P10247*, *EZR-AS1*, *PRLB*, *PVT1*, *ATB*, *NEAT1*, *AC026904.1*, *MEG3*, *XIST*, and *PDCD4-AS1*. However, we analyzed all elevated lncRNAs using ENCORI and UALCAN database and found that only *TMPO-AS1* was overexpressed in *BRCA* patient compared with normal, as shown in Figure 8A-B, further correlation was optimized by using OncoDB database and we found that *TMPO-AS1* was significantly

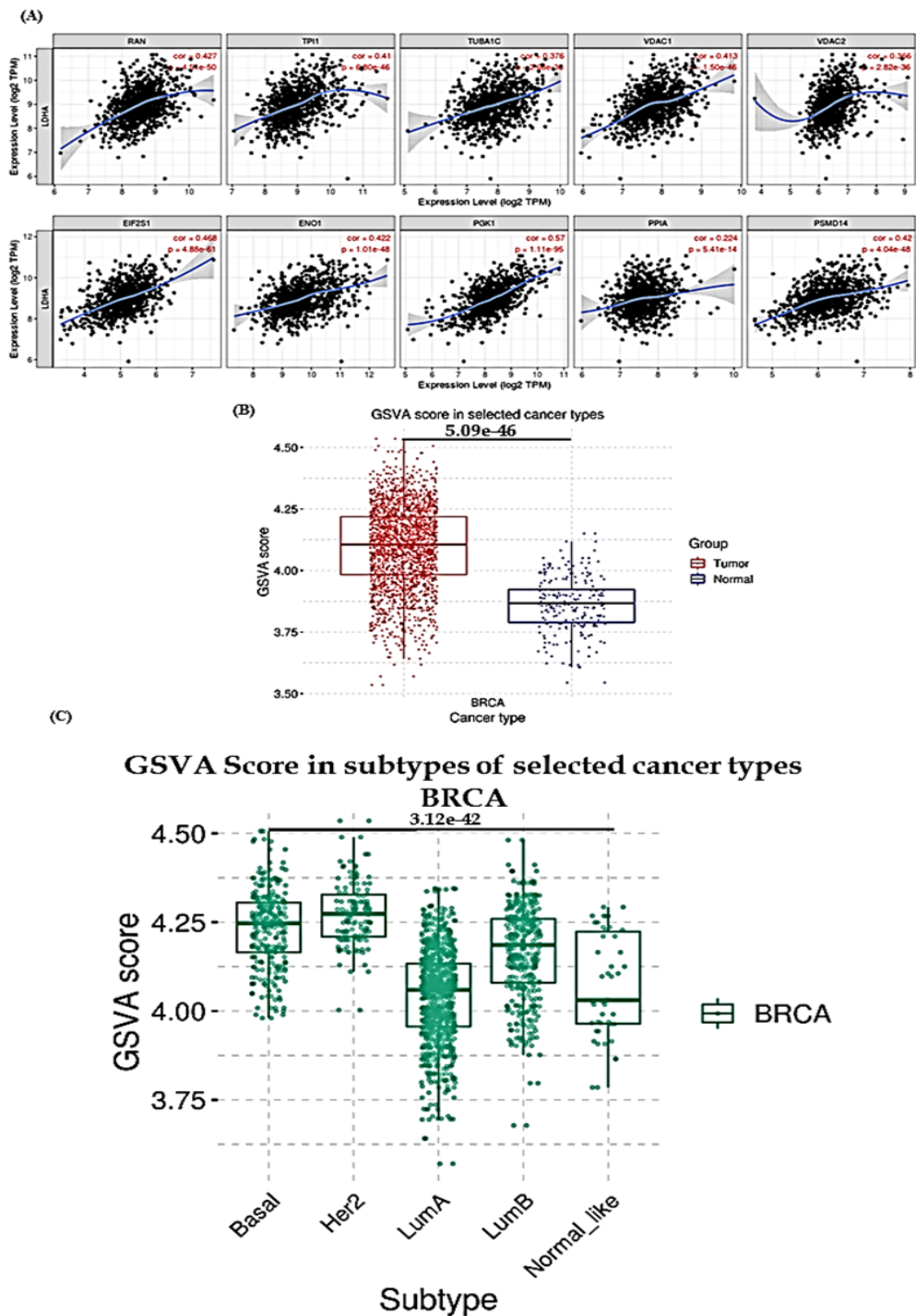


Figure 6. (A) Expression correlation between *LDHA* and top 10 co-expressed genes by using TIMER 2.0. Expression Pattern of all co-expressed genes in breast cancer (B) Tumor vs Normal (C) Subtypes of BRCA using GSCA.

correlated with *LDHA* and *HIF1A* gene in *BRCA* patients as shown in Figure 8C-D. Interestingly, we also found that *TMPO-AS1* was significantly negative correlated with has-miR-383-5p in *BRCA* patients as shown in Figure 8E ( $r = -0.066$  and  $p = 3.06e-02$ ). TANRIC and UALCAN repositories showed that *TMPO-AS1*, a non-coding RNA, was overexpressed in the basal subtype of triple-negative breast cancer classified by PAM50 analysis, as shown in Figures 8F–G. Based on available data, we believe that *TMPO-AS1*/miR-383-5p/*LDHA*/*HIF1A* feedback plays a role in breast cancer.

*LDHA* Correlates to Tumor Infiltration of Immune Cells (TIICs)

The TISIDB database plays an important role in determining the effectiveness of cancer treatment and patient outcomes. In the study, the relationship between *LDHA* performance and TIIC was analyzed using GSCA and TISDB. Created a heat map including various TIICs, including M1 macrophages, M2 macrophages, M0 macrophages, T follicular helper cells, resting memory CD4 T cells, gamma T cells, CD8 T cells, regulatory T cells, Naive CD4 T brain, resting NK cells, activated mast cells, memory B cells, monocytes, neutrophils,

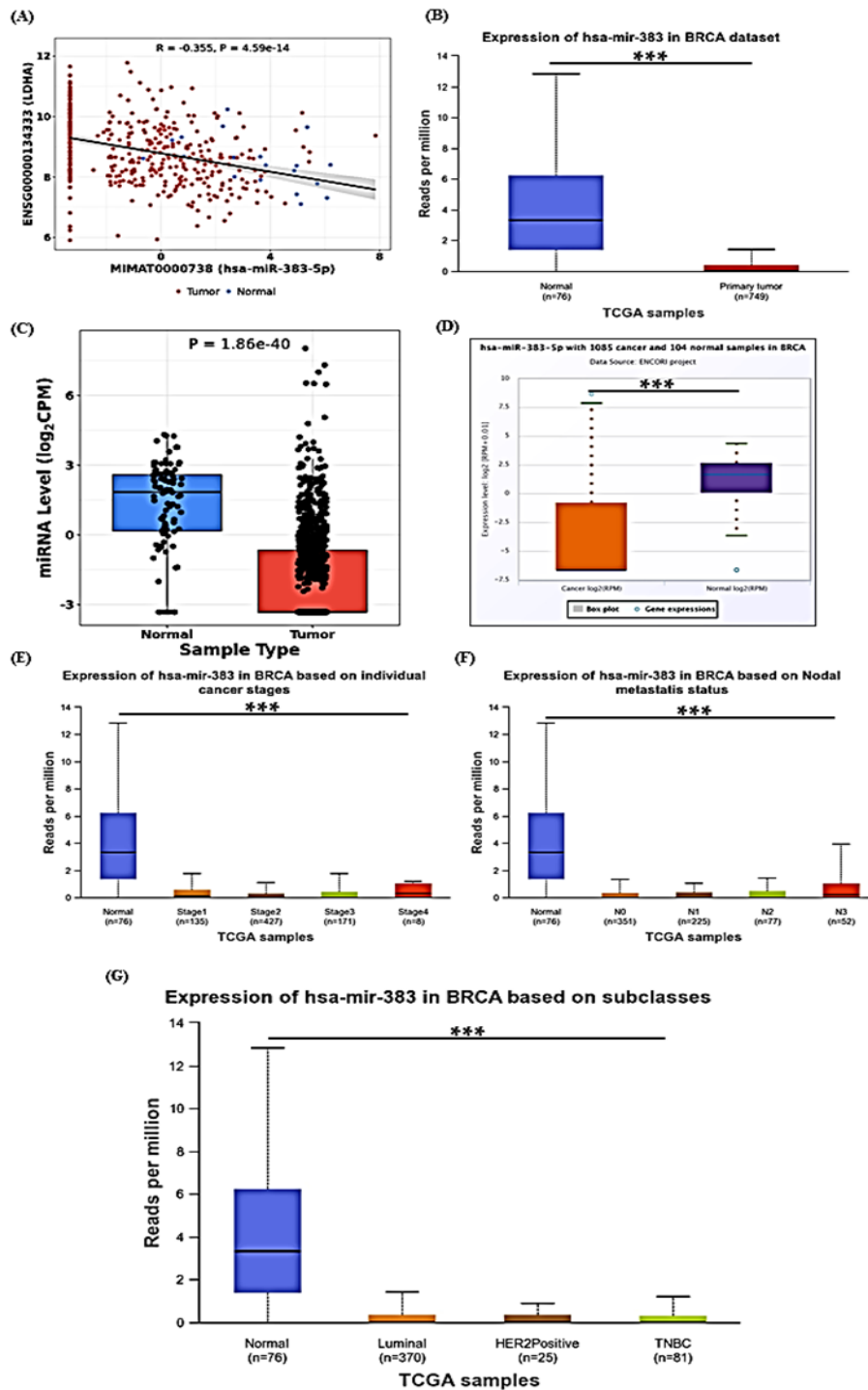


Figure 7. miRNA Expression in Tumor Tissues from Breast Cancer Patients with Various Clinicopathological Features Determined by the UALCAN, and CancerMIRNome Database. A) Boxplot of miR-383, expression according to tumor versus normal (n=76) breast samples (n=749) using UALCAN; (B-C) miR-383-5p expression in Tumor vs Normal using CancerMIRNome; (D) Boxplot of miR-383-5p expression with cancer (n=1085) vs normal (n=104) using ENCORI; (E) Boxplot of miR-383, expression according to normal versus tumor stages (1,2,3 and 4); (F) Boxplot of miR-383, expression according to normal versus tumor from breast cancer patients with different nodal status (N0, N1, N2 and N3). (G) Boxplot of miR-383, expression according to normal versus tumors from patient with different histological subtypes (Luminal, *HER2*<sup>+</sup> and TNBC).

eosinophils, and plasma cells. The heat map of TISIDB data shows that the *LDHA* gene is closely related to the penetration of dendritic cells, especially in breast cancer, as shown in Supplementary Figure 4A-B. Further analysis of GSCA data confirmed this relationship, finding a correlation between *LDHA* expression and Act\_DC

infiltration in the breast (coefficient  $R = 0.44$ ,  $P = 1.9 \times 10^{-55}$ ) as shown in Supplementary Figure 4C. Additionally, *LDHA* and its synergistic gene (*G5VA*) also showed infiltration with Act\_DC with the correlation value,  $R = 0.48$  and  $P = 8.2 \times 10^{-127}$  (Supplementary Figure 4D).

## TMPO-AS1

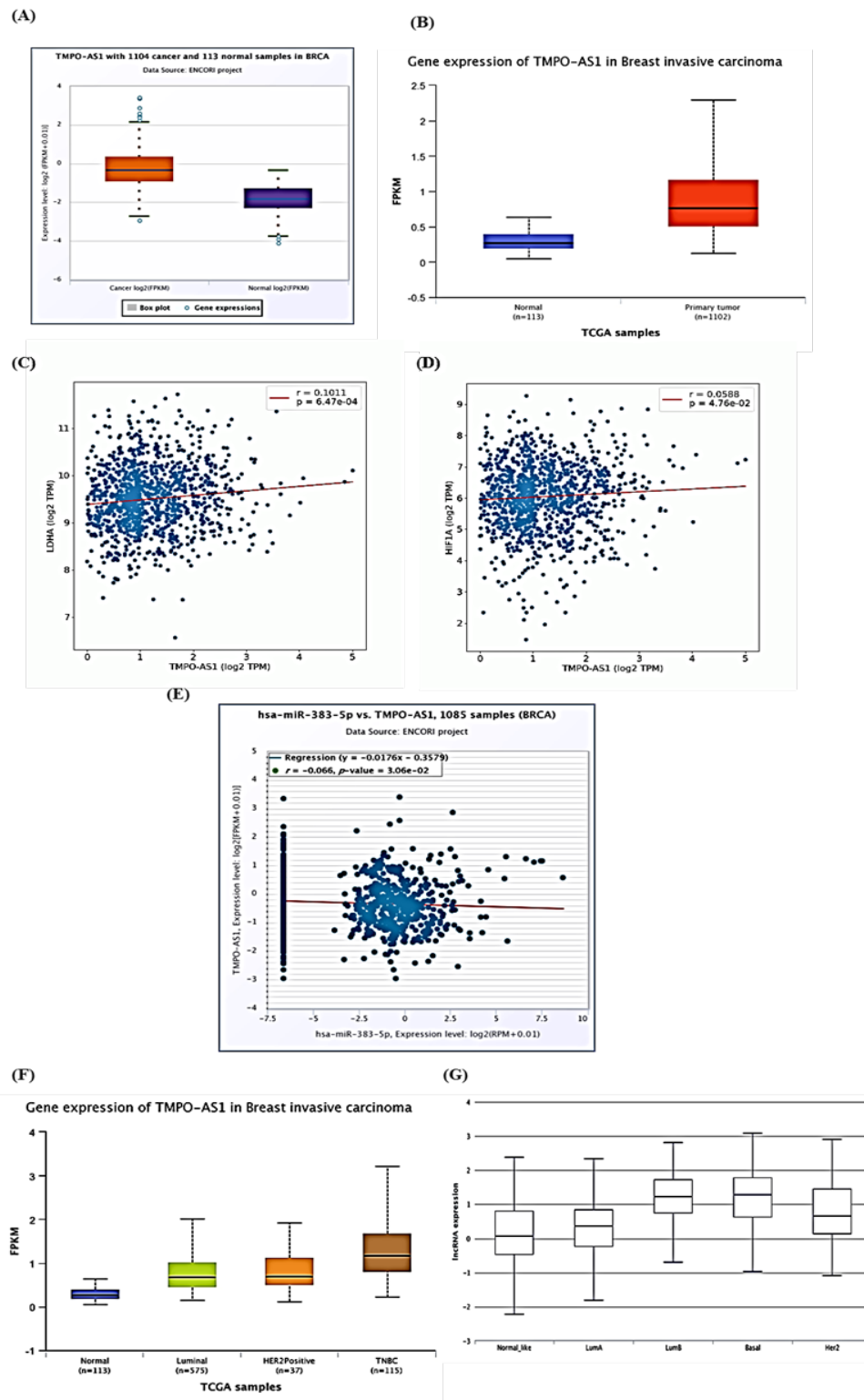


Figure 8. (A) Boxplot of TMPO-AS1 expression in Cancer (n=1104) and normal (n=113) breast cancer samples using ENCORI database; (B) Boxplot TMPO-AS1 gene expression in normal vs tumor using UALCAN; (C) Co-expression of TMPO-AS1 vs LDHA; (D) Co-expression of TMPO-AS1 vs *HIF1A* using OncoDB database; (E) Co-expression of hsa-miR-383-5p vs TMPO-AS1 in breast cancer samples using ENCORI; (F-G) Boxplot of TMPO-AS1, expression according to normal versus tumors from patient with different histological subtypes (Luminal, HER2+ and TNBC).

#### Analysis of protein-ligand interaction between LDHA inhibitors and Withanolide

To be considered a candidate for an inhibitor, it must bind a specific active site cavity with significant binding affinity. For this, the binding mechanisms of the docked

molecules were assessed using LDHA-ligand complexes derived from post-docking analyses. All six ligands were docked both with and without NADH. The binding affinity of all ligands was enhanced in the presence of NADH. The binding affinity of all ligands is summarized



in Table 3. Binding mode shows that the ligands bind in the active site cavity and follow a similar pattern to that of the reference inhibitor (PubChem CID 131955127), as shown in Supplementary Figure 5A. Based on binding affinity and binding pose, Withaferine A and Withanolide D were used for further analysis. Ligand Withaferine A, with a binding affinity of -9.3 kcal/mol, binds in the active site cavity of *LDHA*, forming three H-bonds between the ligand and the amino acids Arg105, Ser195, and His192, as shown in Supplementary Figure 5B. In addition, it also forms five hydrophobic interactions with Pro138, Ile141, Tyr238, Ile241, and Ile325. Withanolide D binds to *LDHA* with a binding energy of -10 kcal/mol. It formed four H-bonds with *LDHA*, two H-bonds formed between Withanolide D and residue Arg105 and Ser195, His192 individually making two H-bonds with ligand, because of the additional H-bond it has a greater binding affinity for *LDHA* as shown in Supplementary Figure 5C. By following a similar interaction pattern as Withaferine A, it forms five hydrophobic interactions with Pro138, Ile141, Tyr238, Ile241, and Ile325.

## Discussion

Breast cancer survival has improved with targeted drugs and hormonal therapy, but high mortality rates persist. New therapeutic biomarkers like CERBB-2 and RTK are being explored for improved patient outcomes [49,50]. Advances in genomics have led to the discovery of genetic targets in cancer research, with *LDHA* expression being a crucial oncogene for tumor growth and metastasis, as highlighted by various studies [51]. Identifying patients with high *LDHA* expression before treatment is important for individualized treatment [52]. Endocrine therapy to eliminate estrogen-dependent cell proliferation has been shown to reduce recurrence and death in most patients with early breast cancer [53]. Liu, Cui, Feng, and Ho have all contributed to the understanding of the role of *LDHA* in breast cancer. *LDHA* is crucial in glucose metabolism and regulates the production of acetyl-CoA, which is essential for EMT-related gene transcription [54–57]. When *LDHA* levels decrease, it inhibits EMT genes and activates autophagy via AMPK signaling. High *LDHA* expression is associated with worse cancer outcomes [56]. Combination chemotherapy is being investigated to improve the therapeutic index of anti-cancer drugs. Targeting cellular metabolism is an interesting method for obtaining specific antibodies without affecting the normal body. *LDHA*, an enzyme crucial in the diagnosis of neoplastic diseases like Hodgkin lymphoma and multiple myeloma [58], was overexpressed in breast cancer cells, metastatic tissues, and brain tumors, leading to shorter survival (RFS) and overall survival compared to OS and distant metastasis-free survival (DMFS). Feng, Yang, and Yadav have all contributed to the understanding of *LDHA*'s role in cancer patient survival, with its increased expression in breast cancer cells, metastatic tissues, and brain tumors [55,59,60].

In addition to using the Human Protein Atlas database, we also found that *LDHA* was overexpressed in breast cancer patients compared to normal subjects,

as shown in Supplementary Figure 3. *LDHA*, a key protein in tumor growth and cell cycle, is linked to various clinicopathological features, including hypoxia and tumor prognosis. Studies by Dong et al. (2023) and Koukourakis (2003) have highlighted the role of *LDHA* in hypoxia, a microenvironmental factor in malignant tumors [61,62]. Chiche et al. (2010) found that *LDHA* catalyzes the last step of glycolysis in hypoxia [63]. HIF-1 and HIF-2, transcriptional regulators, modulate cellular and systemic adaptive responses, affecting genes crucial for tumor growth and cell cycle. This study demonstrates the relationship between *LDHA* and HIF-1 $\alpha$  expression in cancer, and high HIF-1 $\alpha$  expression predicts poor outcomes (RFS, OS, DMFS, and PPS) in cancer patients. Based on gene Gene Ontology using TISIDB database we also found that *LDHA* and its molecular biology associated with Hypoxia as mentioned in Supplementary Table 2. Extensive research has shown that cancer is affected by dysregulation of microRNAs, small non-coding RNA molecules that control gene expression. Dysregulation of miRNAs can occur through various mechanisms, such as DNA amplification, deletions, mutations, epigenetic silencing, or inhibition of miRNA activity. Some known cancer-associated miRNAs include let-7, miR-200 family, miR-10b, miR-21, miR-335, miR-301, miR-155, miR-34a, and miR-205 [64,65]. In our study, we found that the decrease of miRNA miR-383-5p is important in the initiation and development of cancer and increases the risk of cancer. Its overexpression inhibits cell proliferation, migration, and invasion by targeting *LDHA*. TCGA RNAseq data showed that miR-383-5p expression was reduced in breast cancer compared to normal controls. Patients with low miR-383-5p expression have poor differentiation, good tumor metastasis, and high-grade TNM. Using CancerMIRNome data, we also examined the pan-cancer perspective of miR-383-5p and found that miR-383-5p expression was downregulated in all cancer types, including breast cancer, based on ROC analysis (Supplementary Figure 6). Greater molecular heterogeneity is an important problem in breast cancer that affects treatment response and patient prognosis. This study aims to identify genes with high levels of expression (HHE) and their association with prognosis. In this study, the Enrichr repository identified 10 coexpressed genes related to *LDHA* that correlated well with those in the TIMER 2.0 repository. The GSCA and UALCAN databases were used to identify gene expression in breast cancer patients. This shows that there are large changes for each gene. The KM plotter database showed that all seven genes, including the *LDHA* data mean, were associated with poor survival in cancer patients. The Cancer Genome Atlas repository shows that thymopoietin antisense transcript 1 (TMPO-AS1) is a functional lncRNA associated with growth biomarkers in breast and lung cancer. TMPO-AS1 positivity is associated with a poor prognosis in breast cancer patients and is estrogen dependent. TMPO-AS1 appears to be upregulated in MCF-7 cells resistant to endocrine therapy and can be induced by estrogen. It supports the growth and survival of estrogen receptor-positive breast cancer cells in vitro and in vivo. TMPO-AS1 exerts oncogenic functions in

various cancers, such as pancreatic cancer, uterine cancer, non-small cell lung cancer, breast cancer, breast cancer, cancer, and lung adenocarcinoma. It suppresses cancer by targeting the AKT/rapamycin kinase (mTOR) signaling mechanism and suppresses the malignant phenotype of retinoblastoma cells by inhibiting miR-199a-5p, which targets HIF-1 $\alpha$  -LncRNAs and plays an important role in HCC development, such as promoting angiogenic mimicry and increasing cancer cells in HCC. In this study, we also analyzed the expression of TMPO-AS1 in breast cancer and demonstrated its important role in tumor growth. Overexpressed *LDHA* promotes TMPO-AS1 transcription and has been shown to recruit miR-383-5p. This study reveals for the first time the biological role and molecular mechanism of *LDHA*/TMPO-AS1 in TNBC and is expected to identify it as a new therapeutic target.

The tumor microenvironment plays a crucial role in tumor progression to malignant phenotypes, with gene expression in tumor cells and stromal cells influencing their interaction. This study used GSCA and TISIDB data to analyze the relationship between *LDHA* performance and TIICs. Using various TIICs, the *LDHA* gene is closely associated with the entry of Act\_DC Cells especially in *BRCA*. *LDHA*, a health marker, has a significant impact on cancer development, making it a potential therapeutic target in human cancer treatment. Analysis of pathways associated with *LDHA* in breast cancer development reveals potential pathways and genes that can be used as checkpoints to prevent or reduce cancer cells, making them useful biomarkers for effective treatment. Drug Bank was used to measure *LDHA*, and results showed that many chemicals show affinity with *LDHA*, including stiripentol, copper, arteminol, etheno-NAD, nicotinamide, oxamic acid, and etheno-NAD. Stipentol is recommended for its pharmacological and inhibitory activities as mentioned in Supplementary Table 3. In this study we have proposed a natural based alternative i.e. use of withanolides, which has proven to be more affective as compared to chemical based or synthetic based products. In a study conducted by Lacombe et al., they suggested that withanolide D could be a promising radiosensitizer for cancer cells by inhibiting NHEJ pathway and promoting mitotic catastrophe [66]. Very interestingly, in an another study conducted by Chien et al., they showed that withaferine A possess anti- cancer effects by inducing antiproliferation, apoptosis, and DNA damage in an oxidative stress-dependent manner in case of bladder cancer [67]. Also, our study shows that withanolide analogs could be attractive molecules to test *LDHA* inhibition. In silico docking studies predict tight binding of Withaferine A (-9.3kcal/mol) and Withanolide D (-10kcal/mol) by forming hydrogen bonds with *LDHA* active site residues Arg105, Ser195, and His192. These interactions may lead to decrease *LDHA* expression levels in cancer cells.

In conclusion, the study reveals a strong association between *LDHA* expression and HIF-1 $\alpha$  in breast cancer, with *LDHA* expression being inversely associated with miR-383-5p and positively correlated with TMPO-AS1. This suggests that HIF-1 $\alpha$  influences *LDHA* gene expression regulation, potentially promoting breast cancer progression. Overexpression of *LDHA* and HIF-1 $\alpha$

correlates with OS, RFS, DMFS, and PPS in breast cancer patients, suggesting *LDHA* could be a prognostic factor and therapeutic target. *LDHA* mediates the conversion of pyruvate and lactate, and high expression of *LDHA*, HIF-1 $\alpha$ , TMPO-AS1, along with low expression of miR-383-5p is a hallmark of many cancers. It was seen that the sponge formation between TMPO-AS1 and hsa-let-7b-5p may have a significant affect on *LDHA* expression regulation. Due to the sponging effect, the normal functioning of hsa-let-7b-5p gets disrupted, which in turn affects its ability to effectively regulate *LDHA* mRNA levels, in breast cancer. *LDHA* is also closely associated with Act-DC cells, influencing the tumor microenvironment with hypoxia conditions and downregulating miR-383-5p. Withanolide-*LDHA* complexes, esp. withaferine A and withanolide D, exhibit strong binding interactions with *LDHA* and could be prominent scaffolds to develop potential small-molecule inhibitors to decrease the *LDHA* expression level for the development of highly effective therapeutics against breast cancer.

## Author Contribution Statement

Conception: RN, AK, SKS. Interpretation, or analysis of data: RN, PV, JS, SKS, AK. Preparation of the manuscript: RN, PV, JS, SKS, AK and, Supervision: RN, AK, SKS.

## Acknowledgements

### Funding Support

This work is supported by MUJ Endowment Fund E3/2023-24/QE-04-05 to RN and Department of Biotechnology, Govt. of India grant BT/PR40197/BTIS/137/68/2023 to SKS. Department of Biosciences, Manipal University Jaipur is supported by DST-FIST (DST/2022/1012) from Govt. of India.

### Data Availability

The data for this in-silico study were sourced from publicly accessible databases. The respective links and references for these datasets are provided the methodology section for transparency and reproducibility.

### Ethical Clearance

Since this study exclusively utilized publicly available online databases for data extraction and analysis, ethical clearance was not required as per institutional guidelines.

### Conflicts of interest

The authors declare that they have no competing interests.

## References

1. Döhner H, Wei AH, Appelbaum FR, Craddock C, DiNardo CD, Dombret H, et al. Diagnosis and management of aml in adults: 2022 recommendations from an international expert panel on behalf of the eln. *Blood*. 2022;140(12):1345-77. <https://doi.org/10.1182/blood.2022016867>.
2. Zhang N, Wu J, Wang Q, Liang Y, Li X, Chen G, et al. Global

- burden of hematologic malignancies and evolution patterns over the past 30 years. *Blood Cancer J.* 2023;13(1):82. <https://doi.org/10.1038/s41408-023-00853-3>.
3. Sasaki K, Ravandi F, Kadia TM, DiNardo CD, Short NJ, Borthakur G, et al. De novo acute myeloid leukemia: A population-based study of outcome in the united states based on the surveillance, epidemiology, and end results (seer) database, 1980 to 2017. *Cancer.* 2021;127(12):2049-61. <https://doi.org/10.1002/cncr.33458>.
  4. Jensen PD. Evaluation of iron overload. *Br J Haematol.* 2004;124(6):697-711. <https://doi.org/10.1111/j.1365-2141.2004.04838.x>.
  5. Alkhateeb AA, Connor JR. The significance of ferritin in cancer: Anti-oxidation, inflammation and tumorigenesis. *Biochim Biophys Acta.* 2013;1836(2):245-54. <https://doi.org/10.1016/j.bbcan.2013.07.002>.
  6. Wang F, Lv H, Zhao B, Zhou L, Wang S, Luo J, et al. Iron and leukemia: New insights for future treatments. *J Exp Clin Cancer Res.* 2019;38(1):406. <https://doi.org/10.1186/s13046-019-1397-3>.
  7. Lebon D, Vergez F, Bertoli S, Harrivel V, De Botton S, Micol JB, et al. Hyperferritinemia at diagnosis predicts relapse and overall survival in younger aml patients with intermediate-risk cytogenetics. *Leuk Res.* 2015;39(8):818-21. <https://doi.org/10.1016/j.leukres.2015.05.001>.
  8. Yan Z, Chen X, Wang H, Chen Y, Chen L, Wu P, et al. Effect of pre-transplantation serum ferritin on outcomes in patients undergoing allogeneic hematopoietic stem cell transplantation: A meta-analysis. *Medicine (Baltimore).* 2018;97(27):e10310. <https://doi.org/10.1097/md.00000000000010310>.
  9. Mahindra A, Bolwell B, Sobecks R, Rybicki L, Pohlman B, Dean R, et al. Elevated pretransplant ferritin is associated with a lower incidence of chronic graft-versus-host disease and inferior survival after myeloablative allogeneic haematopoietic stem cell transplantation. *Br J Haematol.* 2009;146(3):310-6. <https://doi.org/10.1111/j.1365-2141.2009.07774.x>.
  10. Bazuaye GN, Buser A, Gerull S, Tichelli A, Stern M. Prognostic impact of iron parameters in patients undergoing allo-sct. *Bone Marrow Transplant.* 2012;47(1):60-4. <https://doi.org/10.1038/bmt.2011.13>.
  11. Armand P, Sainvil MM, Kim HT, Rhodes J, Cutler C, Ho VT, et al. Does iron overload really matter in stem cell transplantation? *Am J Hematol.* 2012;87(6):569-72. <https://doi.org/10.1002/ajh.23188>.
  12. Dou L, Shi M, Song J, Niu X, Niu J, Wei S, et al. The prognostic significance of c-reactive protein to albumin ratio in newly diagnosed acute myeloid leukaemia patients. *Cancer Manag Res.* 2022;14:303-16. <https://doi.org/10.2147/cmar.S343580>.
  13. Bertoli S, Paubelle E, Bérard E, Saland E, Thomas X, Tavitian S, et al. Ferritin heavy/light chain (fth1/ftl) expression, serum ferritin levels, and their functional as well as prognostic roles in acute myeloid leukemia. *Eur J Haematol.* 2019;102(2):131-42. <https://doi.org/10.1111/ejh.13183>.
  14. Ihlow J, Gross S, Sick A, Schneider T, Flörcken A, Burmeister T, et al. Aml: High serum ferritin at initial diagnosis has a negative impact on long-term survival. *Leuk Lymphoma.* 2019;60(1):69-77. <https://doi.org/10.1080/10428194.2018.1461860>.
  15. Delavigne K, Bérard E, Bertoli S, Corre J, Duchayne E, Demur C, et al. Hemophagocytic syndrome in patients with acute myeloid leukemia undergoing intensive chemotherapy. *Haematologica.* 2014;99(3):474-80. <https://doi.org/10.3324/haematol.2013.097394>.
  16. Zeidan AM, Giri S, DeVeaux M, Ballas SK, Duong VH. Systematic review and meta-analysis of the effect of iron chelation therapy on overall survival and disease progression in patients with lower-risk myelodysplastic syndromes. *Ann Hematol.* 2019;98(2):339-50. <https://doi.org/10.1007/s00277-018-3539-7>.
  17. Hong J, Woo HS, Ahn HK, Sym SJ, Park J, Cho EK, et al. Pre-treatment blood inflammatory markers as predictors of systemic infection during induction chemotherapy: Results of an exploratory study in patients with acute myeloid leukemia. *Support Care Cancer.* 2016;24(1):187-94. <https://doi.org/10.1007/s00520-015-2762-1>.
  18. Kong SG, Jeong S, Lee S, Jeong JY, Kim DJ, Lee HS. Early transplantation-related mortality after allogeneic hematopoietic cell transplantation in patients with acute leukemia. *BMC Cancer.* 2021;21(1):177. <https://doi.org/10.1186/s12885-021-07897-3>.
  19. Akı Ş Z, Suyanı E, Bildacı Y, Çakar MK, Baysal NA, Sucak GT. Prognostic role of pre-transplantation serum c-reactive protein levels in patients with acute leukemia undergoing myeloablative allogeneic stem cell transplantation. *Clin Transplant.* 2012;26(5):E513-21. <https://doi.org/10.1111/ctr.12028>.
  20. Artz AS, Logan B, Zhu X, Akpek G, Bufarull RM, Gupta V, et al. The prognostic value of serum c-reactive protein, ferritin, and albumin prior to allogeneic transplantation for acute myeloid leukemia and myelodysplastic syndromes. *Haematologica.* 2016;101(11):1426-33. <https://doi.org/10.3324/haematol.2016.145847>.
  21. Wells GA, Shea B, O'Connell D, Peterson J, Welch V, Losos M, Tugwell P. The Newcastle-Ottawa Scale (NOS) for assessing the quality of nonrandomised studies in meta-analyses.
  22. Page M, McKenzie J, Bossuyt P, Boutron I, Hoffmann T, Mulrow C, et al. The prisma 2020 statement: An updated guideline for reporting systematic reviews. *BMJ.* 2021;372:n71. <https://doi.org/10.1136/bmj.n71>.
  23. Tachibana T, Andou T, Tanaka M, Ito S, Miyazaki T, Ishii Y, et al. Clinical significance of serum ferritin at diagnosis in patients with acute myeloid leukemia: A yacht multicenter retrospective study. *Clin Lymphoma Myeloma Leuk.* 2018;18(6):415-21. <https://doi.org/10.1016/j.clml.2018.03.009>.
  24. Penack O, Peczynski C, van der Werf S, Finke J, Ganser A, Schoemans H, et al. Association of serum ferritin levels before start of conditioning with mortality after alloset - a prospective, non-interventional study of the ebmt transplant complications working party. *Front Immunol.* 2020;11:586. <https://doi.org/10.3389/fimmu.2020.00586>.
  25. Armand P, Kim HT, Cutler CS, Ho VT, Koreth J, Ritz J, et al. A prognostic score for patients with acute leukemia or myelodysplastic syndromes undergoing allogeneic stem cell transplantation. *Biol Blood Marrow Transplant.* 2008;14(1):28-35. <https://doi.org/10.1016/j.bbmt.2007.07.016>.
  26. Wahlin A, Lorenz F, Fredriksson M, Remberger M, Wahlin BE, Hägglund H. Hyperferritinemia is associated with low incidence of graft versus host disease, high relapse rate, and impaired survival in patients with blood disorders receiving allogeneic hematopoietic stem cell grafts. *Med Oncol.* 2011;28(2):552-8. <https://doi.org/10.1007/s12032-010-9496-1>.
  27. Dudok D, Virijević M. Prognostic significance of serum ferritin levels on initial diagnosis in patients with acute myeloid leukemia. *Srpski medicinski časopis Lekarske komore.* 2021;2(4):362-70.
  28. Yokus O, Herek C, Cinli TA, Goze H, Serin I. Iron overload during the treatment of acute leukemia:



- Pretransplant transfusion experience. *Int J Hematol Oncol.* 2021;10(3):Ijh36. <https://doi.org/10.2217/ijh-2021-0005>.
29. Kanda J, Mizumoto C, Ichinohe T, Kawabata H, Saito T, Yamashita K, et al. Pretransplant serum ferritin and c-reactive protein as predictive factors for early bacterial infection after allogeneic hematopoietic cell transplantation. *Bone Marrow Transplant.* 2011;46(2):208-16. <https://doi.org/10.1038/bmt.2010.108>.
  30. Meyer SC, O'Meara A, Buser AS, Tichelli A, Passweg JR, Stern M. Prognostic impact of posttransplantation iron overload after allogeneic stem cell transplantation. *Biol Blood Marrow Transplant.* 2013;19(3):440-4. <https://doi.org/10.1016/j.bbmt.2012.10.012>.
  31. Cho BS, Jeon YW, Hahn AR, Lee TH, Park SS, Yoon JH, et al. Improved survival outcomes and restoration of graft-vs-leukemia effect by deferasirox after allogeneic stem cell transplantation in acute myeloid leukemia. *Cancer Med.* 2019;8(2):501-14. <https://doi.org/10.1002/cam4.1928>.
  32. Vallejo C, Batlle M, Vázquez L, Solano C, Sampol A, Duarte R, et al. Phase iv open-label study of the efficacy and safety of deferasirox after allogeneic stem cell transplantation. *Haematologica.* 2014;99(10):1632-7. <https://doi.org/10.3324/haematol.2014.105908>.
  33. Hughes PJ, Marcinkowska E, Gocek E, Studzinski GP, Brown G. Vitamin d3-driven signals for myeloid cell differentiation--implications for differentiation therapy. *Leuk Res.* 2010;34(5):553-65. <https://doi.org/10.1016/j.leukres.2009.09.010>.
  34. Paubelle E, Zylbersztejn F, Alkhaeir S, Suarez F, Callens C, Dussiot M, et al. Deferasirox and vitamin d improves overall survival in elderly patients with acute myeloid leukemia after demethylating agents failure. *PLoS One.* 2013;8(6):e65998. <https://doi.org/10.1371/journal.pone.0065998>.
  35. Yang Y, Tang Z, An T, Zhao L. The impact of iron chelation therapy on patients with lower/intermediate ipss mds and the prognostic role of elevated serum ferritin in patients with mds and aml: A meta-analysis. *Medicine (Baltimore).* 2019;98(40):e17406. <https://doi.org/10.1097/md.00000000000017406>.
  36. Zhou L, Zhao B, Zhang L, Wang S, Dong D, Lv H, et al. Alterations in cellular iron metabolism provide more therapeutic opportunities for cancer. *Int J Mol Sci.* 2018;19(5). <https://doi.org/10.3390/ijms19051545>.
  37. Callens C, Coulon S, Naudin J, Radford-Weiss I, Boissel N, Raffoux E, et al. Targeting iron homeostasis induces cellular differentiation and synergizes with differentiating agents in acute myeloid leukemia. *J Exp Med.* 2010;207(4):731-50. <https://doi.org/10.1084/jem.20091488>.
  38. Ihlow J, Gross S, Neuendorff NR, Busack L, Herneth A, Singh A, et al. Clinical outcome of older adults with acute myeloid leukemia: An analysis of a large tertiary referral center over two decades. *J Geriatr Oncol.* 2021;12(4):540-9. <https://doi.org/10.1016/j.jgo.2020.11.001>.
  39. Jeon SR, Lee JW, Jang PS, Chung NG, Cho B, Jeong DC. Anti-leukemic properties of deferasirox via apoptosis in murine leukemia cell lines. *Blood Res.* 2015;50(1):33-9. <https://doi.org/10.5045/br.2015.50.1.33>.
  40. Isidori A, Loscocco F, Visani G, Chiarucci M, Musto P, Kubasch AS, et al. Iron toxicity and chelation therapy in hematopoietic stem cell transplant. *Transplant Cell Ther.* 2021;27(5):371-9. <https://doi.org/10.1016/j.jct.2020.11.007>.
  41. Fujisawa K, Takami T, Matsumoto T, Yamamoto N, Yamasaki T, Sakaida I. An iron chelation-based combinatorial anticancer therapy comprising deferoxamine and a lactate excretion inhibitor inhibits the proliferation of cancer cells. *Cancer Metab.* 2022;10(1):8. <https://doi.org/10.1186/s40170-022-00284-x>.
  42. Gharagozloo M, Khoshdel Z, Amirghofran Z. The effect of an iron (iii) chelator, silybin, on the proliferation and cell cycle of jurkat cells: A comparison with desferrioxamine. *Eur J Pharmacol.* 2008;589(1-3):1-7. <https://doi.org/10.1016/j.ejphar.2008.03.059>.
  43. Zeidner JF, Karp JE, Blackford AL, Smith BD, Gojo I, Gore SD, et al. A phase ii trial of sequential ribonucleotide reductase inhibition in aggressive myeloproliferative neoplasms. *Haematologica.* 2014;99(4):672-8. <https://doi.org/10.3324/haematol.2013.097246>.
  44. Tarantini F, Cumbo C, Anelli L, Zagaria A, Conserva MR, Redavid I, et al. Exploring the potential of eltrombopag: Room for more? *Front Pharmacol.* 2022;13:906036. <https://doi.org/10.3389/fphar.2022.906036>.
  45. Frey N, Jang JH, Szer J, Illés Á, Kim HJ, Ram R, et al. Eltrombopag treatment during induction chemotherapy for acute myeloid leukaemia: A randomised, double-blind, phase 2 study. *Lancet Haematol.* 2019;6(3):e122-e31. [https://doi.org/10.1016/s2352-3026\(18\)30231-x](https://doi.org/10.1016/s2352-3026(18)30231-x).



This work is licensed under a Creative Commons Attribution-Non Commercial 4.0 International License.